Front. Earth Sci. 2021, 15(1): 23–37
https://doi.org/10.1007/s11707-020-0847-8

RESEARCH ARTICLE

Projection of temperature and precipitation under SSPs-RCPs Scenarios over northwest China

Jiancheng QIN[1,2,3], Buda SU (✉)[1], Hui TAO[1], Yanjun WANG[4], Jinlong HUANG[4], Tong JIANG (✉)[1,4]

1 State Key Laboratory of Desert and Oasis Ecology, Xinjiang Institute of Ecology and Geography, Chinese Academy of Sciences, Urumqi 830011, China
2 College of Resource and Environment Sciences, Xinjiang University, Urumqi 830046, China
3 University of Chinese Academy of Sciences, Beijing 100049, China
4 Collaborative Innovation Center on Forecast and Evaluation of Meteorological Disasters/Institute for Disaster Risk Management/School of Geographical Sciences, Nanjing University of Information Science & Technology, Nanjing 210044, China

Abstract Climate change significantly affects the environmental and socioeconomic conditions in northwest China. Here we evaluate the ability of five general circulation models (GCMs) from 6th phase of the Coupled Model Inter-comparison Project (CMIP6) to reproduce regional temperature and precipitation over northwest China from 1961 to 2014, and project the future temperature and precipitation during 2021 to 2100 under SSPs-RCPs (SSP1-1.9, SSP1-2.6, SSP2-4.5, SSP3-7.0, SSP4-3.4, SSP4-6.0 and SSP5-8.5). The results show that the CMIP6 models can simulate temperature better than precipitation. Projections show that the annual mean temperature will further increase under different SSPs-RCPs scenarios in the 21st century. Future climate changes in the near-term (2021–2040), mid-term (2041–2060) and long-term (2081–2100) are analyzed relative to the reference period (1995–2014). In the long term, warming will be significantly higher than the near and mid-terms. In the long term, annual mean temperature will increase by 1.4°C, 1.9°C, 3.3°C, 5.5°C, 2.7°C, 3.8°C and 6.0°C under SSP1-1.9, SSP1-2.6, SSP2-4.5, SSP3-7.0, SSP4-3.4, SSP4-6.0 and SSP5-8.5, respectively. Spatially, warming in the Junggar Basin will be higher than those in the Tarim Basin. Seasonally, the maximum warming zone will be in the mountainous areas of Tarim Basin during spring and autumn, in the southern basin during winter, and in the east during summer. Precipitation shows an increasing trend under different SSPs-RCPs in the 21st century. In the long term, increase in precipitation will be significantly higher than in the near and mid-terms. Increase in annual precipitation in the long term will be 4.1% under SSP1-1.9, 13.9% under SSP1-2.6, 28.4% under SSP2-4.5, 35.2% under SSP3-7.0, 6.9% under SSP4-3.4, 8.9% under SSP4-6.0, and 27.3% under SSP5-8.5 relative to the reference period of 1995–2014. Spatially, precipitation increase will be higher in the south than the north, especially higher in mountainous regions than the basin under SSP2-4.5, SSP3-7.0, and SSP5-8.5. Seasonally, highest increase can be expected for winter, followed by spring, with significant increase in mountainous regions of southern Tarim Basin. Summer precipitation will reduce in Tian Shan and basins but will significantly increase in the northern margin of the Kunlun Mountain.

Keywords temperature, precipitation, projection, SSPs-RCPs, northwest China

1 Introduction

According to the Fifth Assessment Report of the Intergovernmental Panel on Climate Change, global average surface air temperature will increase by 0.3°C to 4.8°C at the end of 21st century relative to the reference period of 1986–2005 (IPCC, 2013). Many observation and climate model based studies also indicate that global warming is accelerating due to the human factors (Zhou et al. 2014; IPCC, 2013). Regional temperature has experienced a significant increase in China since the late 20th century (Li et al., 2010a; Zhou et al., 2020). Previous studies have shown that response to global warming is different regionally and thus, temperature and precipitation changes vary spatially (Hulme, 1996; Ma et al., 2012). Increase in temperature in northern China is greater than the south during the 20th century, and warming will

Received June 4, 2019; accepted October 15, 2020

E-mails: subd@cma.gov.cn (Buda SU); jiangtong@nuist.edu.cn (Tong JIANG)

accelerate during the 21th century throughout China but with faster speed over northern China (Zhou et al., 2006). For precipitation, north China is turning drier but central China is getting wetter in summer, and southern and east-central China is getting wetter in winter since the mid- 20th century (Hu et al., 2003; Liu et al., 2011; Ma et al., 2012). Recent studies have shown that the arid area is one of the specific regions strongly affected by global warming (Hsiang et al., 2011; Chen et al., 2011). In contrast to the warming and drying trends in most arid areas of the world, the climate in northwest China has become warmer and more humid in recent decades (Shi et al., 2003; Shi et al., 2007).

Northwest China is located in the middle latitudes of Eurasia, where the ecological environment is extremely fragile and adaptation to climate change is relatively weak. As the supply of water resources under changing conditions is a limiting factor for ecological security and socio-economic development of northwest China, response to global warming in northwest China has been of major focus (Li et al., 2012a and 2013). The trends in annual mean temperature and precipitation have been rising in northwest China since 1950 (Zhang et al., 2019). Temperature has an obvious warming trend, and the rate of increase of northwest China is higher in the north than the south. Warming is the most significant in winter. Since the mid-1980s, climate in arid China has undergone a transition from warm dry to warm wet and has led to gradual improvement of vegetation (Shi et al., 2003 and 2007). The increase in the annual precipitation range in the Tarim Basin is larger than other areas and a decreasing trend is observed in the Junggar Basin. Precipitation increase in Junggar Basin is mostly during winter and summer, while that in the Tarim Basin is mainly during spring and summer (Hu et al., 2001; He et al., 2011).

As compare to the reference period of 1986–2005, significant increases of annual mean temperature and precipitation are projected over northwest China (Jiang et al., 2009). Warming will continue in the 21st century and will increase by 4°C to 5.4°C in the long term. Seasonally, summer temperature will increase by 5.6°C, and winter temperature will increase by 5.4°C in the long term (Yu et al., 2015). Precipitation will increase by about 16% in the long term, in terms of winter it will increase by 15% to 32% and in summer there will be a decreasing trend (Yu et al., 2015). This decrease in the south will be obvious in the mountainous area, and increases slightly in the basins by about 3% in the long term (La et al., 2019; Yu et al., 2015; Yu et al., 2017). Change in the climate variables such as temperature and precipitation have a strong impact on the fragile ecosystem such as in northwest China, which are highly sensitive to local hydrological cycles and water supply/demand (Piao et al., 2010; Fang et al., 2013). Previous studies on future climate change in northwest China depended mainly on phase three and five of the Coupled Model Inter-comparison Project (CMIP) (Yu et al., 2017; La et al., 2019). Currently, a new set of coordinated climate model experiments have been conducted in phase six of the Coupled Model Inter-comparison Project (CMIP6). The new phase of CMIP involves more modeling groups with improved climate models, and is expected to provide more reliable projections (Eyring et al., 2016). The CMIP6 has been applied to project climate change and its impact on ocean and economy (Chen et al., 2020; Na et al., 2020; Lin et al., 2020; Tokarska et al., 2020). In this paper, we evaluate the ability of CMIP6 models in reproducing the 20th century temperature and precipitation over northwest China, and simulate the future spatiotemporal changes in annual and seasonal temperature and precipitation under combined scenarios of Shared Socio-economic Pathways and Representative Concentration Pathways (SSPs-RCPs), with the aim to provide support for understanding the impacts of climate change over northwest China. Understanding the changes in these climate variables is critical to assess the effects of future climate change on the ecological and socioeconomic systems in northwest China. Research on climate variability and climate change in northwest China is a necessity in order to transfer scientific knowledge to decision-making processes.

2 Study area

The study area (73°–97°E, 33°–50°N) covers an area of approximately 1.6 million km^2 in China. Being far away from the coast and surrounded by Kunlun, Tian Shan, and Altay mountains, temperate continental climate dominates here (Fig. 1(a)). The annual mean temperature ranges from 4°C to 8°C in Junggar Basin and from 10°C to 13°C in Tarim Basin (Fig. 1(b)). The annual precipitation over Junggar Basin and Ili Valley ranges between 100 and 500 mm, while Tarim Basin receives only 20–100 mm (Fig. 1(c)). The world second largest shifting sand desert, i.e. the Taklamakan Desert, located in the Tarim Basin (Tao et al., 2017).

3 Methodology

3.1 Data source

Simulation of climate during the 20th century by the CMIP6 is known as historical experiments, which is forced by greenhouse gases, aerosols, land use, volcanoes, and solar radiation, etc. The purpose of historical experiments is to evaluate the performance of the general circulation models (GCMs) on the current climate conditions. Observed temperature and precipitation during 1961–2014 are from CN05.1 grid data (Wu and Gao, 2013), which was generated using the ground-based 2400 stations and has been widely applied in the field of climate change

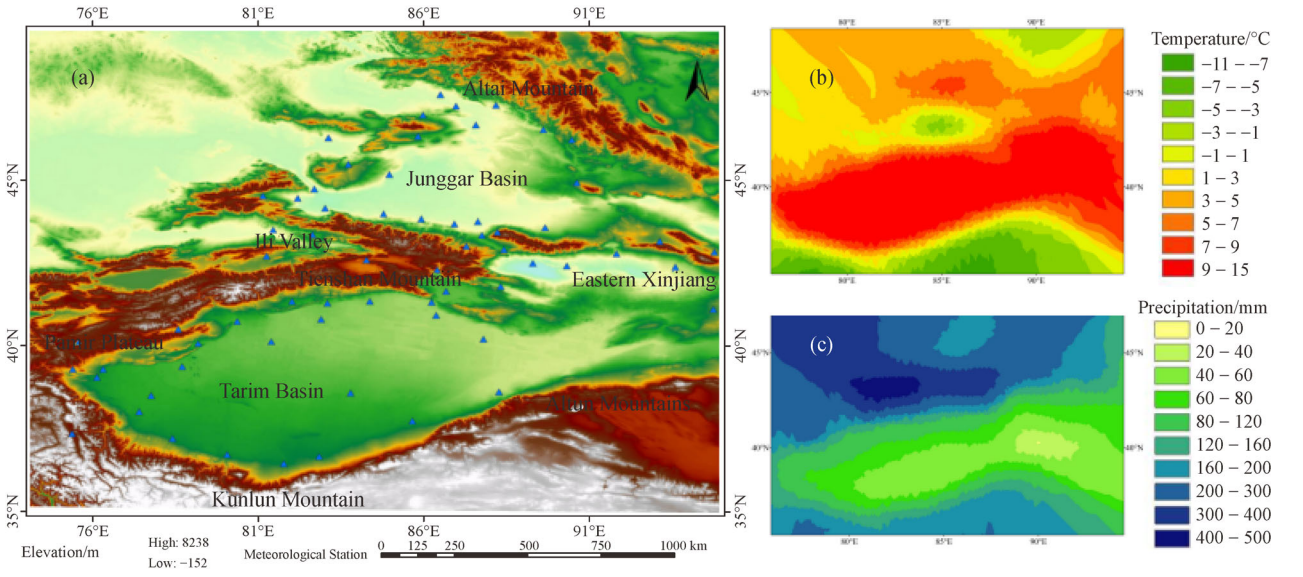

Fig. 1 Location and spatial patterns of temperature and precipitation of the study area.

impact research (Tian et al., 2015).

3.2 Climate models

Output from five climate models (Table 1) were selected for the climate change projections under SSPs-RCPs, which include SSP1-1.9, SSP1-2.6, SSP2-4.5, SSP3-7.0, SSP4-3.4, SSP4-6.0, and SSP5-8.5 scenarios. The SSP1-1.9 scenario reflects most closely a 1.5 °C emissions concentration under the Paris Agreement. For SSP1-2.6, the total radiative forcing has a peak of about 2.6 Wm^{-2} around the year 2050 and then decreases. In SSP2-4.5 and SSP4-3.4, the total radiative forcing will rise until 2070 and then have a stable concentrations (without an overshoot pathway to 4.5 and 3.4 Wm^{-2}). SSP3-7.0, SSP4-6.0, and SSP5-8.5 are the medium-high reference scenarios where radiative forcing level are approximately 7.0, 6.0, and 8.5 Wm^{-2} by the end of the 21st century (Meinshausen et al., 2020). In this study, future climate changes in near-term (2021–2040), mid-term (2041–2060) and long-term (2081–2100) are analyzed relative to the reference period (1995–2014). For future projections, the multi-model ensemble (MME) is more reasonable than a single model (Xu and Xu, 2012). Thus, projections on temperature and precipitation in northwest China are derived from a multi-model ensemble (MME) of the five GCMs.

3.3 Simulation assessment

Spatial correlation coefficient (COR), the bias (BIAS) and the root mean square error (RMSE) are widely applied to evaluate the simulation of CMIP models (Su et al., 2016, Zhu et al., 2019). These parameters are defined as

$$COR=\frac{\sum_{i=1}^{N}(X_{i\_fd1}-\overline{X_{i\_fd1}})(X_{i\_fd2}-\overline{X_{i\_fd2}})}{\sqrt{\sum_{i=1}^{N}((X_{i\_fd1}-\overline{X_{i\_fd1}}))^2\sum_{i=1}^{N}((X_{i\_fd2}-\overline{X_{i\_fd2}})^2}}, \quad (1)$$

$$BIAS=\frac{1}{t}\sum_{n=1}^{t}(M_n-O_n)=\overline{M}-\overline{O}, \quad (2)$$

$$RMSE=\left[\frac{1}{t}\sum_{n=1}^{t}(M_n-O_n)^2\right]^{\frac{1}{2}}, \quad (3)$$

where, X_{i_fd1} (X_{i_fd2}) denotes the value of field1(field2) at grid point i, $\overline{X_{i\_fd1}}$, $\overline{X_{i\_fd2}}$ denotes the mean of all the grid points in field1(field2), N denotes the total number of grid

Table 1 List of CMIP6 models used in this study

Name	Modeling group	Original resolution (lon × lat)
CanESM5	Centre for Climate Modeling and Analysis, Canada	2.81° × 2.81°
CNRM-ESM2-1	National Centre for Scientific Experiments, France	1.25° × 2.5°
IPSL-CM6A-LR	Institute Pierre Simon Laplace, France	1.25° × 2.5°
MIROC6	Atmosphere and Ocean Research Institute, Japan	1.4° × 1.4°
MPI-ESM2-0	Planck Meteorological Institute, Germany	0.93° × 0.93°

points in the field (Gao et al., 2012), M_n denotes climate model data sets, O_n denotes the observed data sets, t denotes the number of the sample. Student's t test was used to detect the significance of changing temperature and precipitation (Wei, 1999).

3.4 EDCDF method

The systematic bias between simulations and observations is corrected by applying the equidistant cumulative distribution functions matching method (EDCDF) and statistically downscaled to a common 0.5° × 0.5° grid (Su et al., 2016). The EDCDF method developed by Li et al. (2010b) applies a quantile-based mapping of the CDFs between both the historic and projection period and matches the climatic fields in the future projection period. The EDCDF method is a widely used bias correction for many studies (Su et al., 2016; Yang et al., 2018; Zhu et al., 2019; Wang et al., 2019). The formula for EDCDF is given as:

$$x_{m_p/adj} = x_{m-p} + F_{o-c}^{-1}(F_{m-p}(x_{m-p})) - F_{m-c}^{-1}(F_{m-p}(x_{m-p})), \quad (4)$$

where X is the variable, F is the CDF, $o-c$ is the historical measured value, while m-c is the simulated value during the baseline period, m-p is the forecasted value during the future, and $X_{m\text{-}p}$, adj is the bias-corrected value. A normal distribution is fitted to temperature fields. Due to the intermittent feature of precipitation in nature, a mixed gamma distribution considering the months with no rain is fitted to precipitation fields. The CDF for precipitation is written as:

$$P(x) = (1-P)f(x) + PF(x), \quad (5)$$

where, k is the percentage of months with precipitation, $h(x)$ is 0 when there is no precipitation or 1 when there is precipitation, $F(x)$ is the CDF for the time series with precipitation, a two-parameter gamma distribution is fitted to the time series with precipitation.

4 Results

4.1 Performance of climate models

We compared the observations and simulations before and after the bias-correction during 1961–2014. As shown in Fig. 2, the original GCM outputs underestimate the annual mean temperature but overestimate the annual precipitation. Temperature bias of individual model simulations from the observations varies from −5.7°C to 4.2°C. Precipitation bias of individual model simulations from the observations varies from 2.8 to 221.6 mm. The spatial correlation coefficient of simulated and observed temperature and precipitation varies from 0.77 to 0.91 and 0.47 to 0.68, respectively (Table 2).

The EDCDF method was applied to correct the deviation of the GCM outputs from observation. Results show that the bias-correction can dramatically reduce the bias of the GCM outputs compared to the original simulations. After correction, the MME can capture the low temperature centers in Kunlun, Tian Shan, and Altai mountain regions, and the high temperature centers in the Tarim Basin and the Junggar Basin. The MME can also reasonably reproduce spatial distribution of annual precipitation, which is relatively high in mountain areas (exceeding 200 mm) and low in the Tarim River Basin (< 50 mm) (Fig. 2).

The EDCDF method shows remarkable skill in reducing the bias of original model-simulated temperature and precipitation, with bias reduced to less than 1°C and 50 mm, respectively. After bias correction, spatial patterns of MME and observed temperature and precipitation can exceed 0.9 (Table 2).

The relative errors between bias-corrected GCM simulations and observed temperature and precipitation during 1961–2014 show that annual mean temperature is 4.94°C by MME of GCMs, which is less by 0.05°C from observed; and annual precipitation is simulated as 150.9 mm, less by 0.9 mm from observation. Both the annual mean temperature and annual precipitation illustrate increasing trends for 1961–2014. Increase rate is 0.3°C/10a and 6.4 mm/10a based on observation and 0.2°C/10a and 4.2 mm/10a by MME. The results of bias-corrected MME are consistent with the observations with relatively small errors. In terms of the slope rate, GCM could do better for temperature simulation than precipitation (Fig. 3).

Figure 4 depicts the Taylor diagrams of annual mean temperature and annual precipitation. It is clear that all bias-corrected GCMs are in phase with observation, with correlation coefficients varying in the range 0.8–0.9 and RMS error of 0.2–0.5. The RMS error of MME is lower than the single GCM, and MME has a higher correlation.

4.2 Temperature

4.2.1 Temporal changes in annual mean temperature

Figure 5 shows the variation of annual mean temperature by GCMs for 1961–2100. It is quite clear that temperature rises sharply after the mid-1980s, and continuous warming will be projected in the future. For SSP1-1.9 and SSP1-2.6, annual mean temperature will continuously rise until 2050 and begin to cool slightly thereafter, with slope of 0.49°C/10a and 0.51°C/10a during 2021–2050, and 0.3°C/10a and 0.39°C/10a during 2051–2100. Under SSP2-4.5 and SSP4-3.4 scenarios, temperature will continuously rise until 2085 and then effectively stabilize after 2085, with slope of

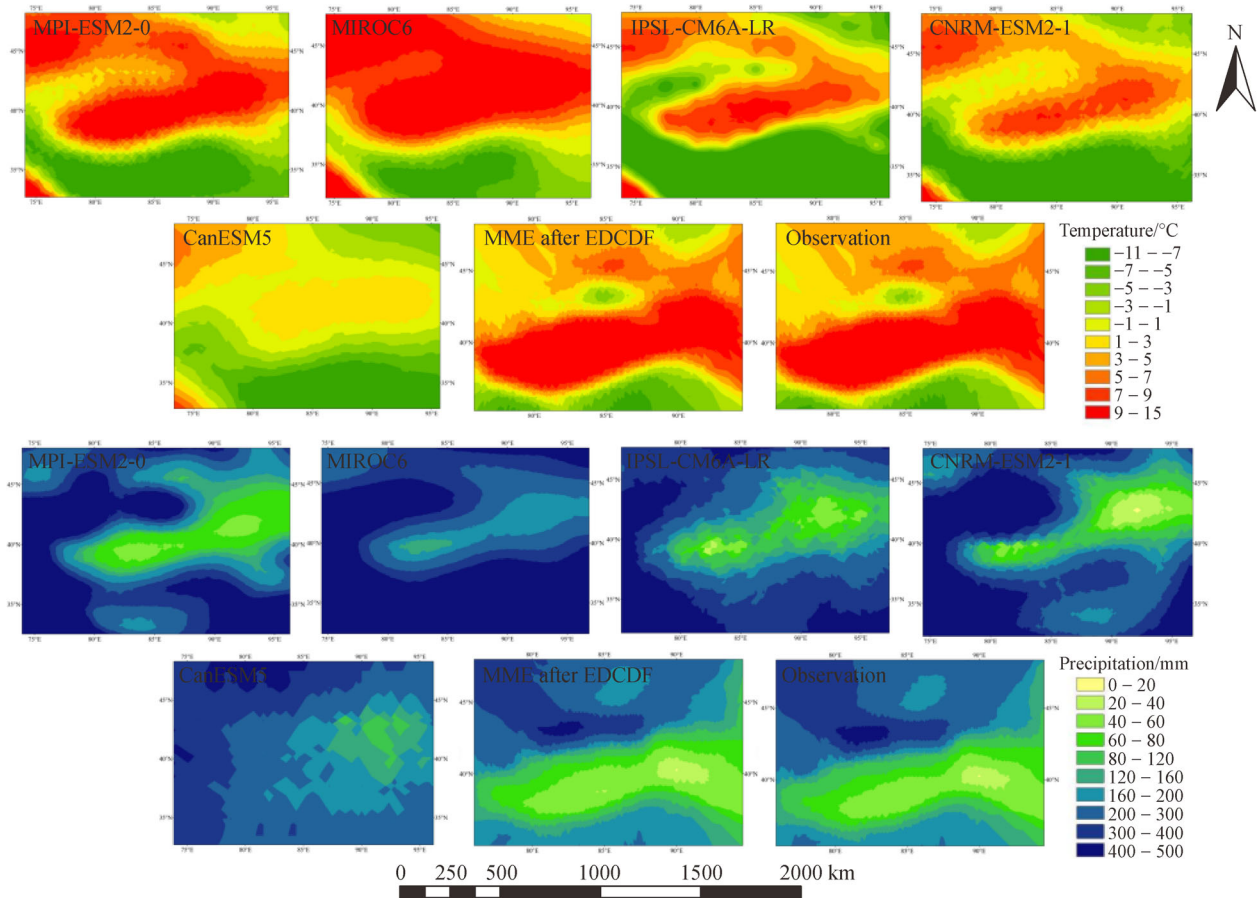

Fig. 2 Spatial patterns of observed and simulated temperature and precipitation during the reference period (1961–2014).

Table 2 Correlation coefficient of CMIP6 model outputs and observations

		CanESM5	CNRM-ESM2-1	IPSL-CM6A-LR	MIROC6	MPI-ESM2-0
Temperature	Original outputs	0.77	0.89	0.85	0.84	0.91
	Bias-corrected	0.97	0.99	0.96	0.98	0.99
Precipitation	Original outputs	0.68	0.67	0.59	0.47	0.66
	Bias-corrected	0.98	0.95	0.98	0.99	0.99

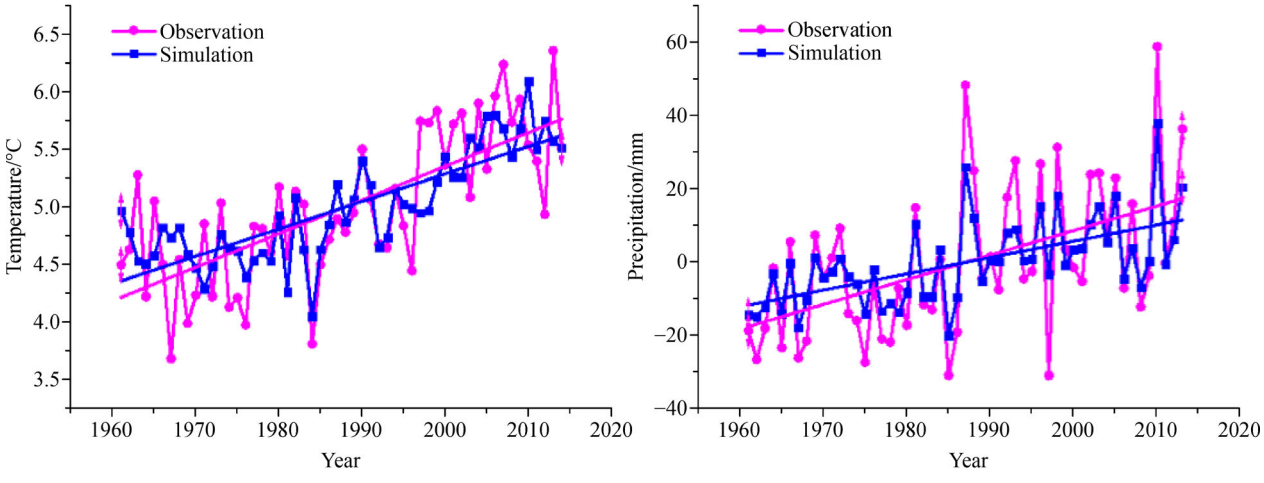

Fig. 3 Variations of temperature and precipitation by the observation and multi-model ensemble mean during baseline period (1961–2014).

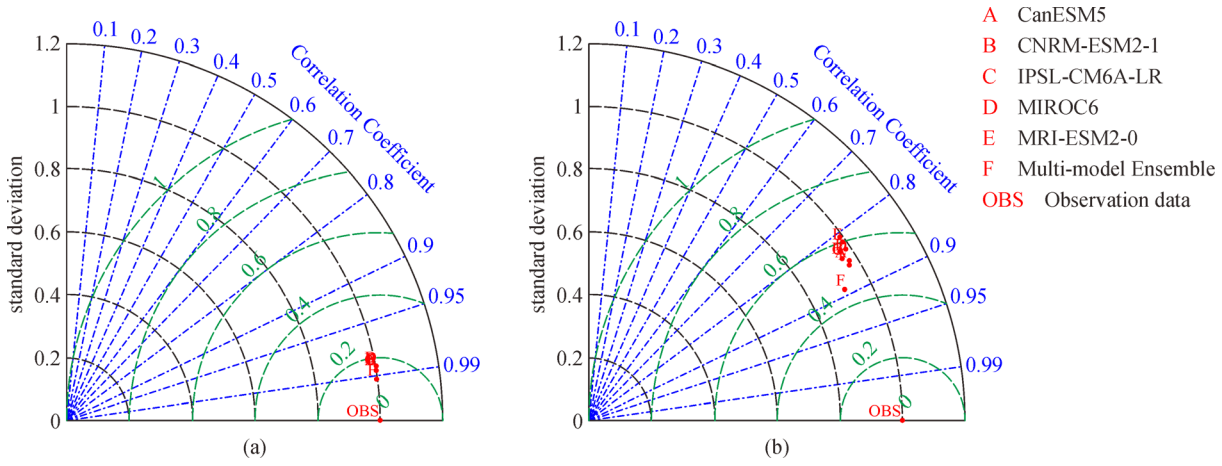

Fig. 4 Taylor diagram of (a) temperature and (b) precipitation for CMIP6 models compared to observations (1961–2014).

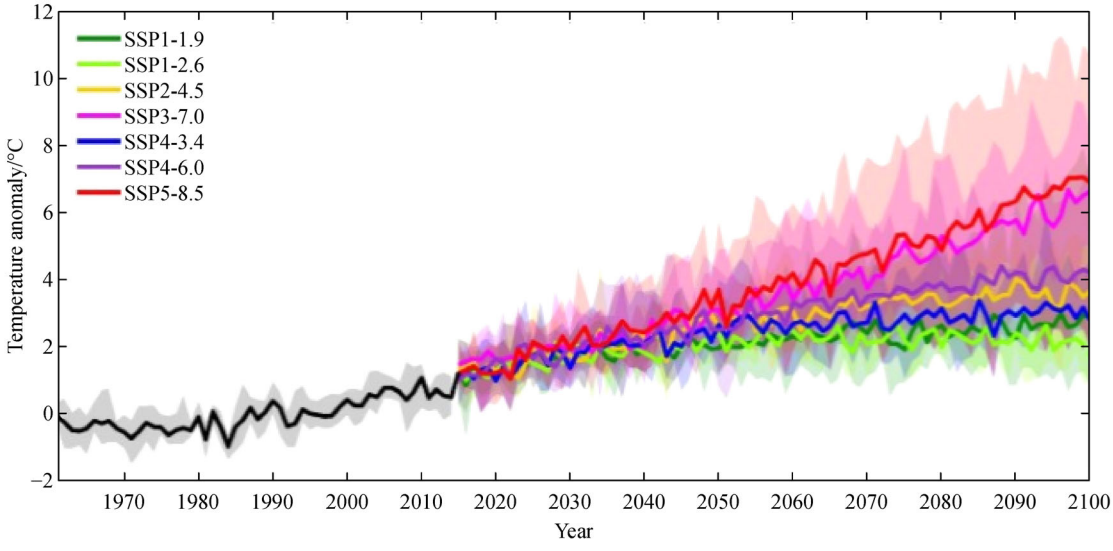

Fig. 5 Temporal changes in annual mean temperature during 1961–2100 under SSPs-RCPs (relative to 1995–2014).

0.37°C/10a and 0.33°C/10a during 2021–2085, and –0.06°C/10a and –0.08°C/10a during 2085–2100. For SSP3-7.0, SSP4-6.0 and SSP5-8.5, temperature will rise continuously with the ongoing increase of radiative forcing. The warming tendency for 2021–2100 will be 0.18°C/10a for SSP1-1.9, 0.22°C/10a for SSP1-2.6, 0.31°C/10a for SSP2-4.5, 0.43°C/10a for SSP3-7.0, 0.27°C/10a for SSP4-3.4, 0.34°C/10a for SSP4-6.0, and 0.47°C/10a for SSP5-8.5.

4.2.2 Spatial changes in annual mean temperature

To better present the temporal and spatial variation of warming, we classified SSPs-RCPs as low (SSP1-1.9 and SSP1-2.6), medium (SSP2-4.5 and SSP4-3.4) and high (SSP3-7.0, SSP4-6.0, and SSP5-8.5) emissions scenarios. Relative to 1995–2014, warming rate stays at the same levels of approximately 1.6°C under all SSPs-RCPs in the near-term. Under SSP1-1.9 and SSP1-2.6 scenarios, areal averaged warming will be approximately 1.6°C and 2.0°C in the mid-term, slightly higher than that of 1.4°C, and 1.9°C in the long term. Under SSP2-4.5 and SSP4-3.4, warming in the mid-term will be approximately 2.6°C and 2.3°C, which is less than that of 3.3°C and 2.7°C in the long term. It should be noted that temperature will grow dramatically under SSP3-7.0, SSP4-6.0, and SSP5-8.5, and reach approximately 5.5°C, 3.8°C, and 6.0°C in the long term, remarkably greater than that of 3°C, 2.7°C, and 3.4°C in the mid-term (Table 3).

We select SSP1-1.9, SSP2-4.5, and SSP5-8.5 to represent the low, medium, and high emissions scenarios, respectively. Figure 6 shows the spatial distributions of temperature changes under SSP1-1.9, SSP2-4.5, and SSP5-8.5 in the near-term, mid-term, and long-term

relative to the reference period (1995–2014). Comparison of annual mean temperature in the future horizons with that in the reference period by Student's *t*-test shows that the changes are statistically significant at the 95% confidence level in entire regions, with warming in the northern part greater than the south.

In the near-term, warming will be approximately 1.6°C under all SSPs-RCPs. In the mid-term, annual mean temperature will increase by 2°C–3°C, with warming in some parts of Altun Mountain above 3°C. In the long term, increase in the annual mean temperature will be more than 4.5°C. In particular, temperature in the mountainous regions of southern Tarim Basin will increase by 5°C–6°C.

4.2.3 Seasonal changes in annual mean temperature

The air surface temperature will increase all the year around, with the greatest increases of 2.1°C, 2.6°C, 4.0°C, 5.9°C, 3.3°C, 4.6°C, and 6.7°C in summer, followed by autumn (1.8°C, 2.4°C, 3.9°C, 6.2°C, 3.2°C, 4.2°C, and 6.7°C), spring (1.6°C, 2.1°C, 3.3°C, 5.1°C, 2.8°C, 3.7°C, and 5.7°C), and the smallest increases of 1.3°C, 1.8°C, 3.1°C, 5.7°C, 2.7°C, 3.6°C, and 6.1°C in winter during 2081-2100 compared to the reference period (1995–2014), respectively, under SSP1-1.9, SSP1-2.6, SSP2-4.5, SSP3-7.0, SSP4-3.4, SSP4-6.0, and SSP5-8.5 (Table 4). Take SSP2-4.5 as an example, under which the world will follow the current development model, linear trends of spring, summer, autumn and winter temperature will be 0.34°C/10a, 0.4°C/10a, 0.38°C/10a, and 0.30°C/10a during 2021–2100. In the near-, mid- and long-terms, air surface temperature will increase by 1.8°C, 3.2°C, and 3.3°C in spring, 2.2°C, 3.6°C, and 4.0°C in summer, 2.0°C, 3.5°C, and 3.9°C in autumn and 1.4°C, 2.7°C, and 3.1°C in winter under SSP2-4.5. Overall, relative to 1995–2014, warming will be the largest under SSP5-8.5, followed by

Table 3 Temperature changes with relative to 1995-2014 under SSPs-RCPs (°C)

	SSP1-1.9	SSP1-2.6	SSP2-4.5	SSP3-7.0	SSP4-3.4	SSP4-6.0	SSP5-8.5
2021–2040	1.5	1.5	1.6	1.7	1.5	1.7	1.8
2041–2060	1.6	2.0	2.6	3.0	2.3	2.7	3.4
2081–2100	1.4	1.9	3.3	5.5	2.7	3.8	6.0

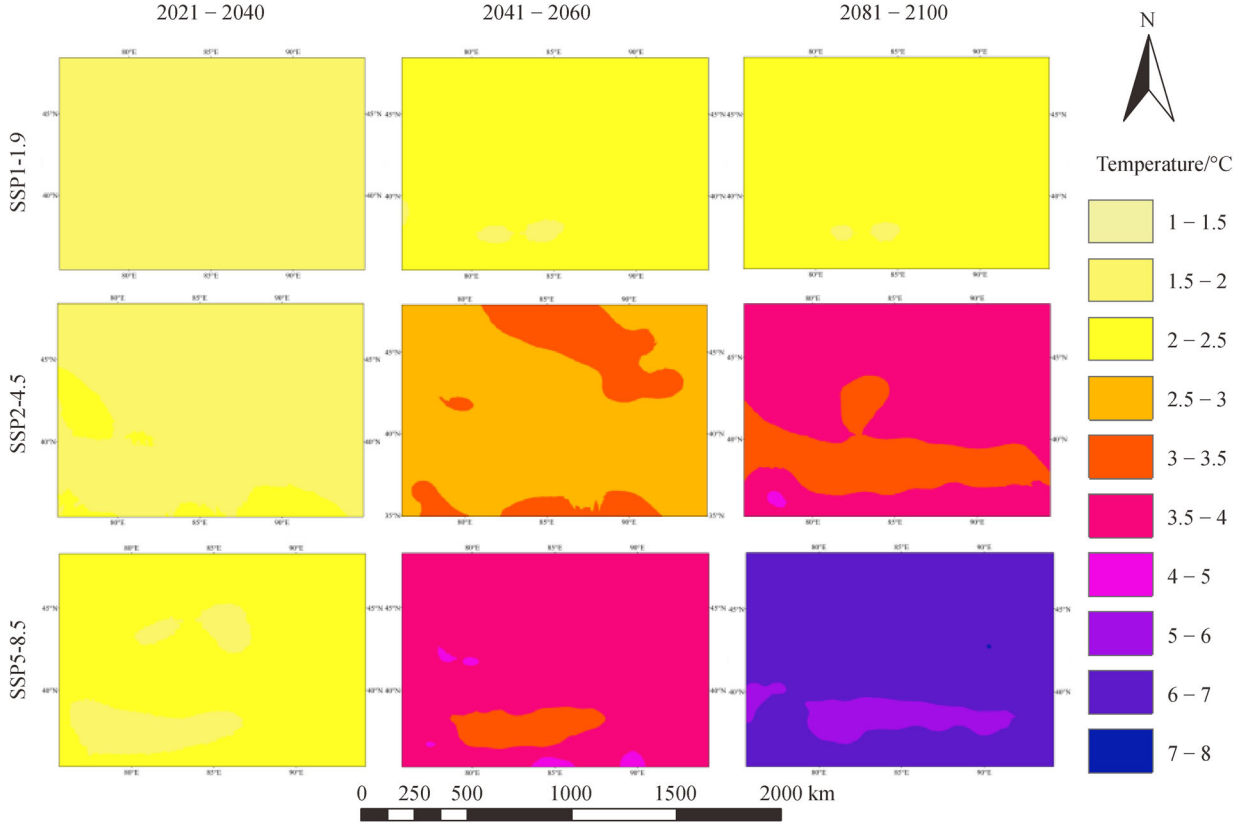

Fig. 6 Spatial patterns of temperature changes in periods of 2021–2040, 2041–2060 and 2081–2100 relative to the reference period (1995–2014) under SSP1-1.9, SSP2-4.5, and SSP5-8.5.

SSP 3-7.0, and SSP 1-1.9 will be the smallest.

Spatially, changes in seasonal temperature will be similar to the annual in all three time horizons. Warming will be the main characteristic of seasonal temperatures in the near-, mid- and long-term under SSPs-RCPs. In the long term, warming will be significantly higher than the near and mid-terms. Warming in summer and autumn will be relatively larger, followed by winter and spring. In spring, warming of Tarim Basin will be higher than the Junggar Basin, and the maximum warming zone will be in the north foot of Kunlun Mountain. In summer, warming of Junggar Basin will be high in the Tarim Basin, and the maximum warming zone will be in the eastern Xinjiang (Fig. 7). In autumn, spatial pattern of warming will be similar to the spring, but generally about 1°C higher. During winter, spatial distribution in warming will be similar to autumn, but with the maximum warming zone in the Tarim Basin.

4.3 Precipitation

4.3.1 Temporal changes in annual precipitation

Figure 8 shows the percentage change of annual precipitation during 1961–2100 relative to 1995–2014. Annual precipitation will increase under all SSPs-RCPs before 2060, with linear trend of 1.6%/10a, 3.2%/10a, 4.3%/10a, 5.1%/10a, 0.52%/10a, 0.96%/10a, and 2.7%/10a, respectively, under SSP1-1.9, SSP1-2.6, SSP2-4.5, SSP3-7.0, SSP4-3.4, SSP4-6.0, and SSP5-8.5. After 2060, trends in annual precipitation will be differentiated for different scenarios. It is projected to increase slightly from 2060 to 2100 with a trend of approximately 1.7%/10a, 1.8%/10a, and 2.2%/10a, respectively, under SSP1-1.9, SSP4-3.4, and SSP4-6.0, respectively. Meanwhile, annual precipitation will keep an increase rate of 3.8%/10a, and 6.5%/10a under SSP1-2.6 and SSP2-4.5. An even stronger increase is projected with rate of 8.5%/10a and 6.3%/10a during 2060–2100, respectively, under SSP3-7.0 and SSP5-8.5. The areal averaged annual precipitation will increase from 2021 to 2100, with 0.8%/10a for SSP1-1.9, 1.7%/10a for SSP1-2.6, 2.7%/10a for SSP2-4.5, 3.4%/10a for SSP3-7.0, 0.6%/10a for SSP4-3.4, 0.8%/10a for SSP4-6.0, and 2.3%/10a for SSP5-8.5.

4.3.2 Spatial changes in annual precipitation

Relative to the reference period (1995–2014), areal averaged annual precipitation is projected to increase from 2021 to 2100 with obvious higher rates in the south. In general, precipitation changes will vary 0.3%–16.8% in the near-term, 2.7%–25.5% in the mid-term, and 6.9% - 35.2% in the long term under different SSPs-RCPs. In the near-term, increase of annual precipitation will less than 5% under SSP1-1.9, SSP4-3.4, and SSP4-6.0, but will increase by 14.2%, 11%, 16.8%, and 6.7% under SSP2-4.5, SSP1-2.6, SSP3-7.0, and SSP5-8.5, respectively. The areal averaged annual precipitation will increase continuously until the end of 21st century. Under SSP1-1.9, SSP4-3.4, and SSP4-6.0, increases will be 8.6%, 2.7%, and 6.2%, respectively, in the mid-term, and slightly change to 4.1%, 6.9%, and 8.9% respectively, in the long term. Under SSP1-2.6, increases will be 13.5% in the mid-term, and almost remain stable in the long term (approximately 13.9%). It is noteworthy that increases will be stronger under SSP2-4.5, SSP3-7.0, and SSP5-8.5, with rate of 28.4%, 35.2%, and 27.3%, respectively, in the long term, remarkably greater than that of 19.4%, 25.5%, and 14.4% in the mid-term (Table 5).

Spatially, a clear increase in precipitation is projected in the Tarim Basin during 2021–2100, especially in the mountainous regions of southern Tarim Basin, where

Table 4 Seasonal temperature change in periods of 2021–2040, 2041–2060 and 2081–2100 relative to the reference period (1995–2014) under SSPs-RCPs (°C)

		SSP1-1.9	SSP1-2.6	SSP2-4.5	SSP3-7.0	SSP4-3.4	SSP4-6.0	SSP5-8.5
Spring	2021–2040	1.6	1.6	1.8	1.9	1.8	2.0	2.2
	2041–2060	1.7	2.2	3.2	4.0	2.5	3.4	4.2
	2081–2100	1.6	2.1	3.3	5.1	2.8	3.7	5.7
Summer	2021–2040	2.1	2.0	2.2	2.2	2.2	2.2	2.5
	2041–2060	2.2	2.6	3.6	4.3	3.2	3.9	5.1
	2081–2100	2.1	2.6	4.0	5.9	3.3	4.6	6.7
Autumn	2021–2040	1.8	1.8	2.0	2.2	1.9	2.0	2.3
	2041–2060	1.9	2.3	3.5	4.7	3.0	3.7	5.1
	2081–2100	1.8	2.4	3.9	6.2	3.2	4.2	6.7
Winter	2021–2040	1.5	1.5	1.4	1.8	1.5	1.6	1.6
	2041–2060	1.6	1.9	2.7	4.1	2.5	3.2	4.3
	2081–2100	1.3	1.8	3.1	5.7	2.7	3.6	6.1

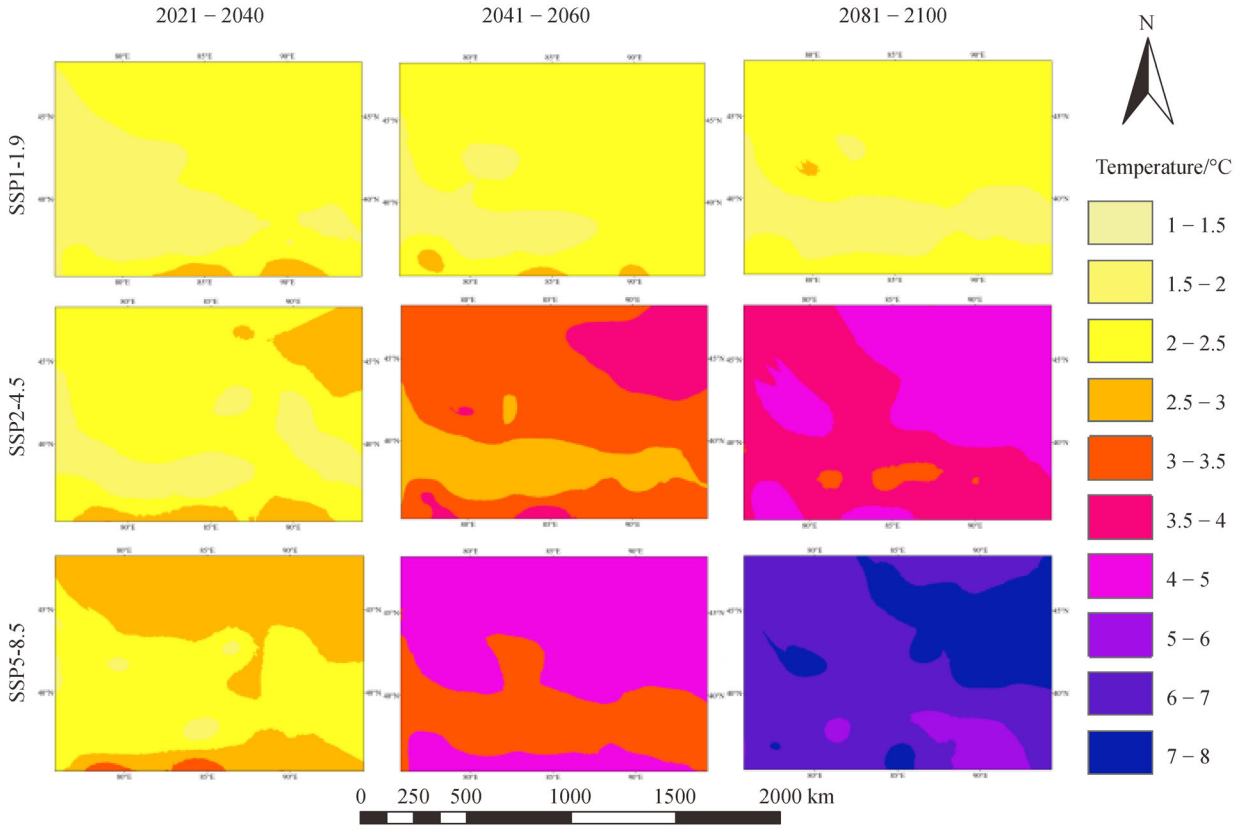

Fig. 7 Spatial patterns of summer temperature change in periods of 2021–2040, 2041–2060 and 2081–2100 relative to the reference period (1995–2014) under SSP1-1.9, SSP2-4.5 and SSP5-8.5.

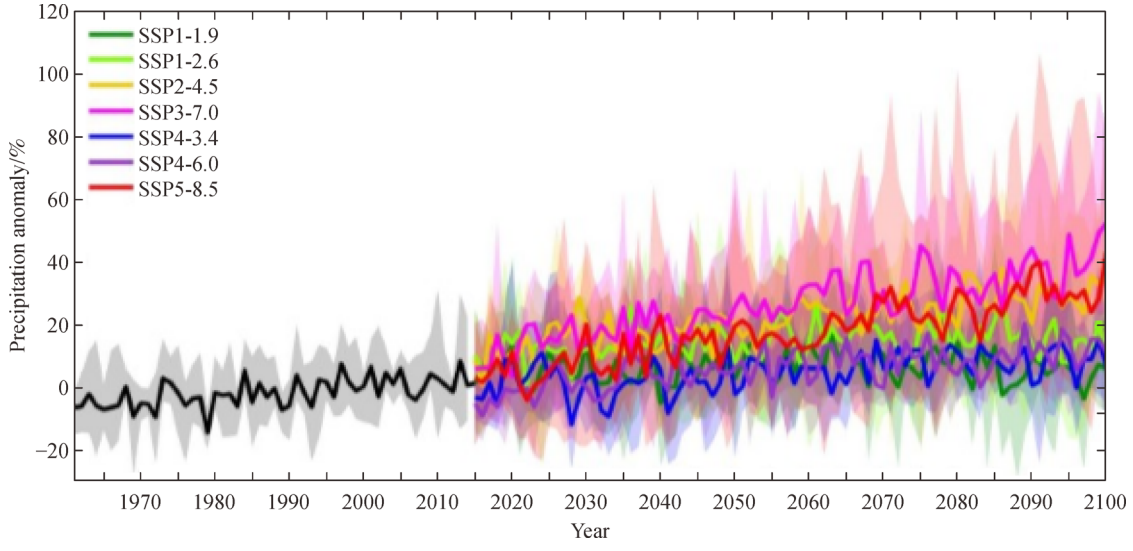

Fig. 8 Temporal changes of annual averaged precipitation during 1961–2100 under SSPs-RCPs (relative to 1995–2014)

increase will be 16%, 24%, 34%, 40%, 7%, 10% and 21%, respectively under SSP1-1.9, SSP1-2.6, SSP2-4.5, SSP3-7.0, SSP4-3.4, SSP4-6.0, and SSP5-8.5 in the near-term, and 9.4%-45.8% in the mid-term. In these areas, increases will be more obvious by the long-term, with rates of 17%, 30%, 48%, 71%, 14%, 19%, and 47% under SSP1-1.9, SSP1-2.6, SSP2-4.5, SSP3-7.0, SSP4-3.4, SSP4-6.0 and SSP5-8.5, respectively. In general, annual precipitation will increase in most areas. In the mountainous regions of southern Tarim Basin there will be significant increase in

Table 5 Percentage change of annual precipitation in the 21st century under SSPs-RCPs with relative to 1995–2014 (%)

	SSP1-1.9	SSP1-2.6	SSP2-4.5	SSP3-7.0	SSP4-3.4	SSP4-6.0	SSP5-8.5
2021–2040	3.9	11.0	14.2	16.8	0.3	0.9	6.7
2041–2060	8.6	13.5	19.4	25.5	2.7	6.2	14.4
2081–2100	4.1	13.9	28.4	35.2	6.9	8.9	27.3

precipitation by above 40% in the long term. While in the basin area, where large area of desert exists, the increase will be limited. The annual precipitation increase in the eastern part of Xinjiang will not be significant, especially in Hami region (Fig. 9).

4.3.3 Seasonal changes in annual precipitation

Average future seasonal precipitation will consistently increase but with evident differences among SSPs-RCP scenarios. With the greatest increases of 23.4%, 39.7%, 78%, 122.3%, 27.4%, 42.8%, and 104.8% in winter, followed by spring (8.5%, 23%, 47%, 60.8%, 11.8%, 16%, and 49.3%), autumn (5.8%, 11.1%, 25.4%, 35.7%, 8.9%, 10.8%, and 27.4%), and the smallest increases of 0.2%, 8.5%, 14.9%, 10.9%, 2.6%, 1.3%, and 6.3% in summer during 2081–2100 compared to the reference period (1995–2014) under SSP1-1.9, SSP1-2.6, SSP2-4.5, SSP3-7.0, SSP4-3.4, SSP4-6.0, and SSP5-8.5, respectively. Take SSP2-4.5 as an example, linear trends of spring, summer, autumn, and winter precipitation will be 4.5%/10a, 1.2%°C/10a, 2.4%/10a, and 7.8%/10a during 2021–2100. In the near, mid- and long-terms, the precipitation will increase by 27.8%, 30.4%, and 47% in spring, 5.5%, 6.5%, and 14.9% in summer, 13.1%, 21.4%, and 25.4% in autumn and 44%, 57.7%, and 78% in winter under SSP2-4.5 (Table 6).

Relative to 1995–2014, precipitation increase will be the highest and most significant in winter, followed by spring and autumn, but decrease in summer (Figs. 10–11). And increase in the long term will be obviously higher than that in the mid- and near-terms. Winter precipitation will significantly increase in the north foot of the Kunlun and Altun mountains, but increase slightly in western Tianshan

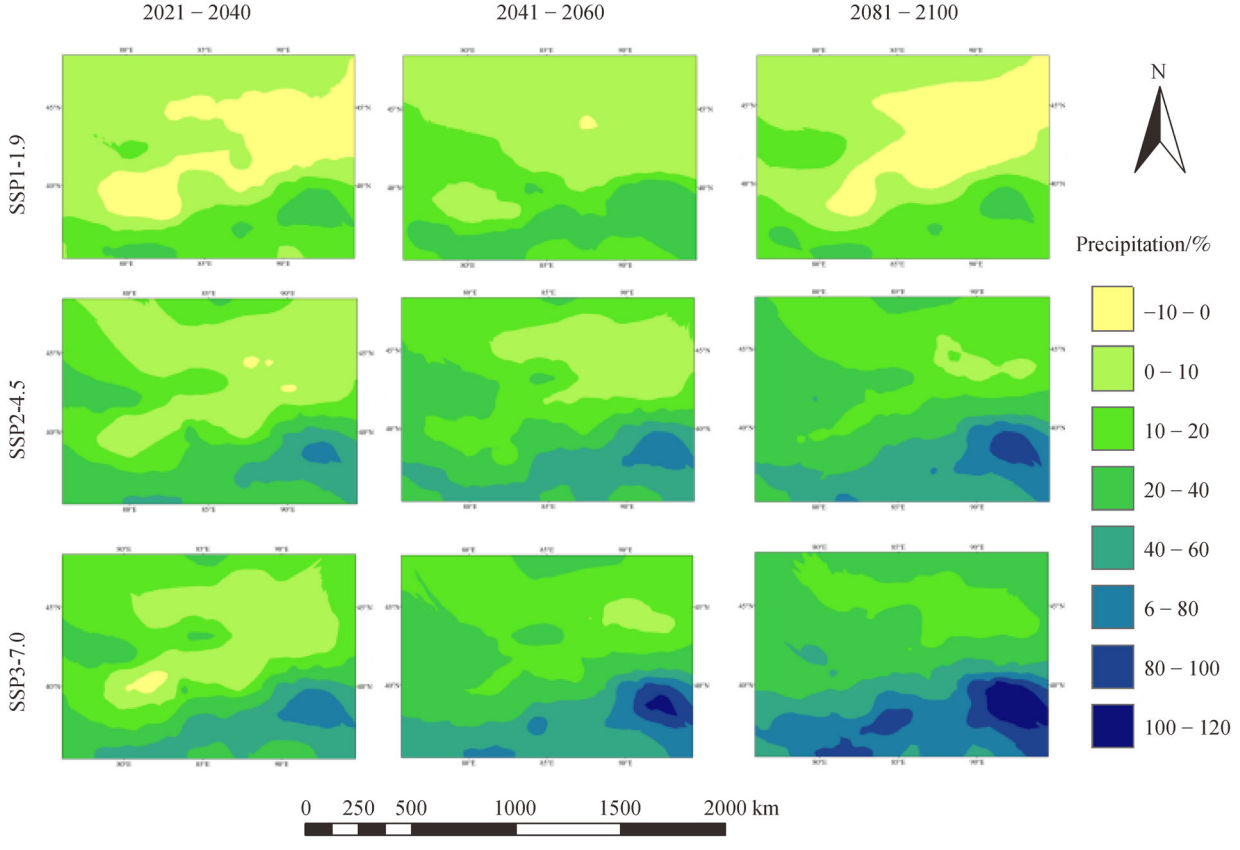

Fig. 9 Spatial patterns of precipitation change in periods of 2021–2040, 2041–2060 and 2081–2100 relative to the reference period (1995–2014) under SSP1-1.9, SSP2-4.5, and SSP3-7.0.

Table 6 Seasonal precipitation changes in periods of 2021–2040, 2041–2060 and 2081–2100 relative to the reference period (1995–2014) under SSPs-RCPs (%)

		SSP1-1.9	SSP1-2.6	SSP2-4.5	SSP3-7.0	SSP4-3.4	SSP4-6.0	SSP5-8.5
Spring	2021–2040	7.7	21.2	27.8	30.6	2.5	2.3	13.1
	2041–2060	11.0	22.6	30.4	38.7	5.9	8.7	27.5
	2081–2100	8.5	23.0	47.0	60.8	11.8	16.0	49.3
Summer	2021–2040	0.1	5.1	5.5	5.0	–1.9	–1.1	–0.4
	2041–2060	3.6	4.3	6.5	6.9	–1.7	1.3	2.3
	2081–2100	0.2	8.5	14.9	10.9	2.6	1.3	6.3
Autumn	2021–2040	8.4	7.2	13.1	19.8	5.7	4.0	10.6
	2041–2060	8.3	15.0	21.4	26.3	3.7	6.9	13.6
	2081–2100	5.8	11.1	25.4	35.7	8.9	10.8	27.4
Winter	2021–2040	18.3	39.4	44.0	56.0	7.5	13.7	35.6
	2041–2060	25.8	40.2	57.7	73.2	19.0	22.6	50.6
	2081–2100	23.4	39.7	78.0	122.3	27.4	42.8	104.8

during 2021–2100. In addition, winter precipitation will significantly increase under SSP2-4.5 and SSP3-7.0 (Fig. 10).

In spring, spatial changes in the near and mid-terms will be similar, with precipitation decrease in eastern Xinjiang but increase in other regions. Precipitation in the mountainous regions of southern Tarim Basin will increase significantly in the long term, and increase in precipitation under SSP2-4.5, SSP3-7.0, and SSP5-8.5 will significantly larger than the other scenarios. In autumn, there will be a

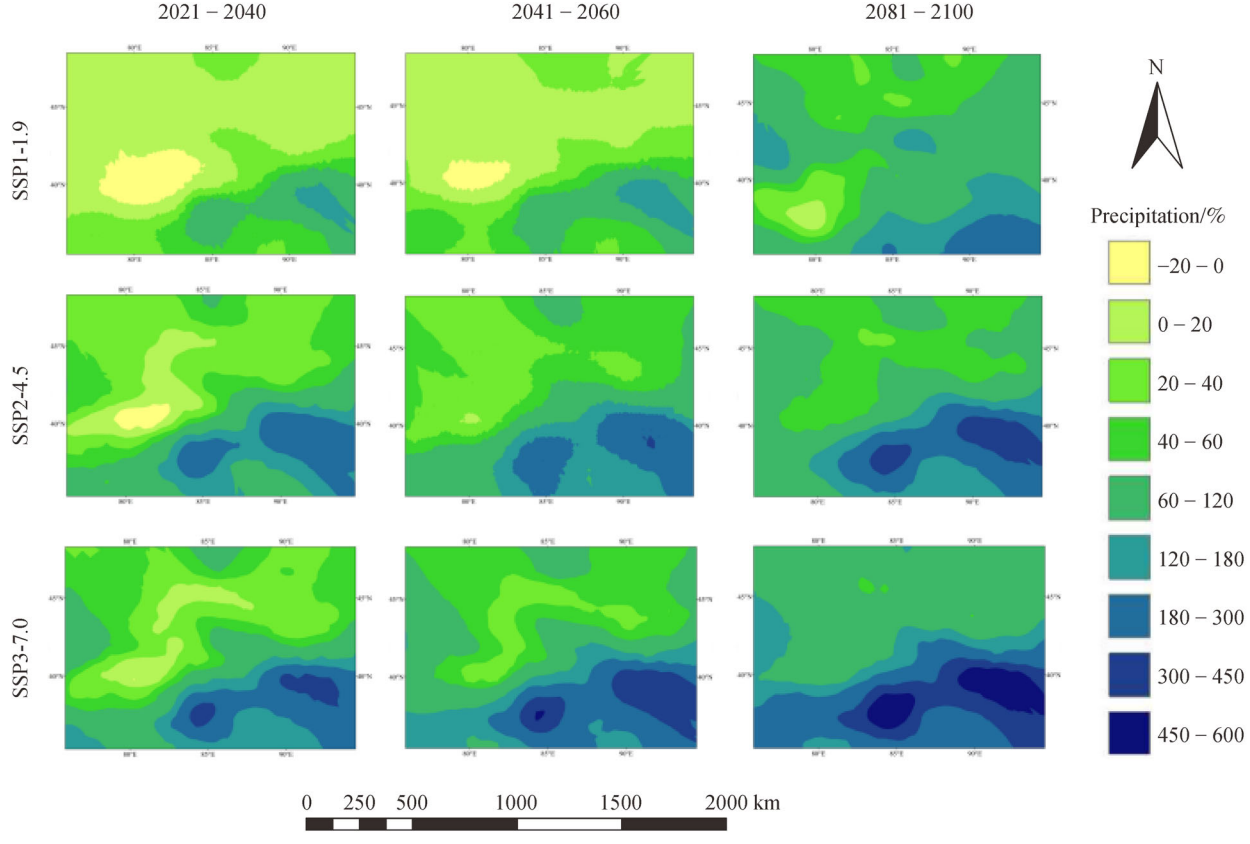

Fig. 10 Spatial patterns of winter precipitation changes in periods of 2021–2040, 2041–2060 and 2081–2100 relative to the reference period (1995–2014) under SSP1-1.9, SSP2-45 and SSP3-7.0.

relatively small increase in precipitation. In all three time horizons, precipitation will be comparatively higher in the mountainous areas than that in the basins. Summer precipitation will significantly decrease in most parts during 2021–2100 except in the southern mountainous areas. The decrease in precipitation in the basin area will be about 10%, and might heavily impact agriculture and the ecosystem. Increase in precipitation will be significant under SSP2-4.5, much larger than the other scenarios (Fig. 11).

5 Discussion

In this study, we evaluate the ability of five GCMs from the CMIP6 in describing temperature and precipitation over northwest China by comparing with ground observations for 1961–2014. We found that multi-model ensemble can capture the temporal and spatial distribution of observed temperature and precipitation in northwest China. Higher greenhouse emission scenarios correspond to high rise in temperature (IPCC, 2013). Projected temperature and precipitation in this study is basically consistent with previous studies (Li et al., 2012b; Yu et al., 2015 and 2017; La et al., 2019). Based on the ensemble from five GCMs, there will be an increase in temperature over northwest China in the 21st century. The maximum warming zone will be in the mountainous areas of southern Xinjiang in spring and autumn, in the Tarim Basin in winter, and will be in the eastern Xinjiang in summer. Projection by CMIP6 will be 0.3°C–0.5°C higher than CMIP5 to the mid- and long-term with increase in precipitation obvious in the south, but comparatively less in the Junggar Basin. Precipitation will significantly increase during the winter, especially in the mountainous regions of southern Xinjiang. There will be comparatively less increase in precipitation in the basin area, but obvious increase in the mountainous areas of Tarim Basin during the spring and autumn, while summer precipitation will slightly reduce in Tian Shan and eastern parts. A larger magnitude of discrepancy can be observed in SSP5-8.5 than SSP2-4.5 both in temperature and precipitation, indicating a stronger response of the climate system to anthropogenic warming.

Previous studies have shown that the warming in northwest China is greater than that in other parts of China (Cheng and Wang, 2006). Increase of temperature in the future can be seen under different SSPs-RCPs scenarios over northwest China. Warming will continue with the ongoing increase of radiative forcing, especially over Junggar Basin. The increasing magnitude under the SSP-

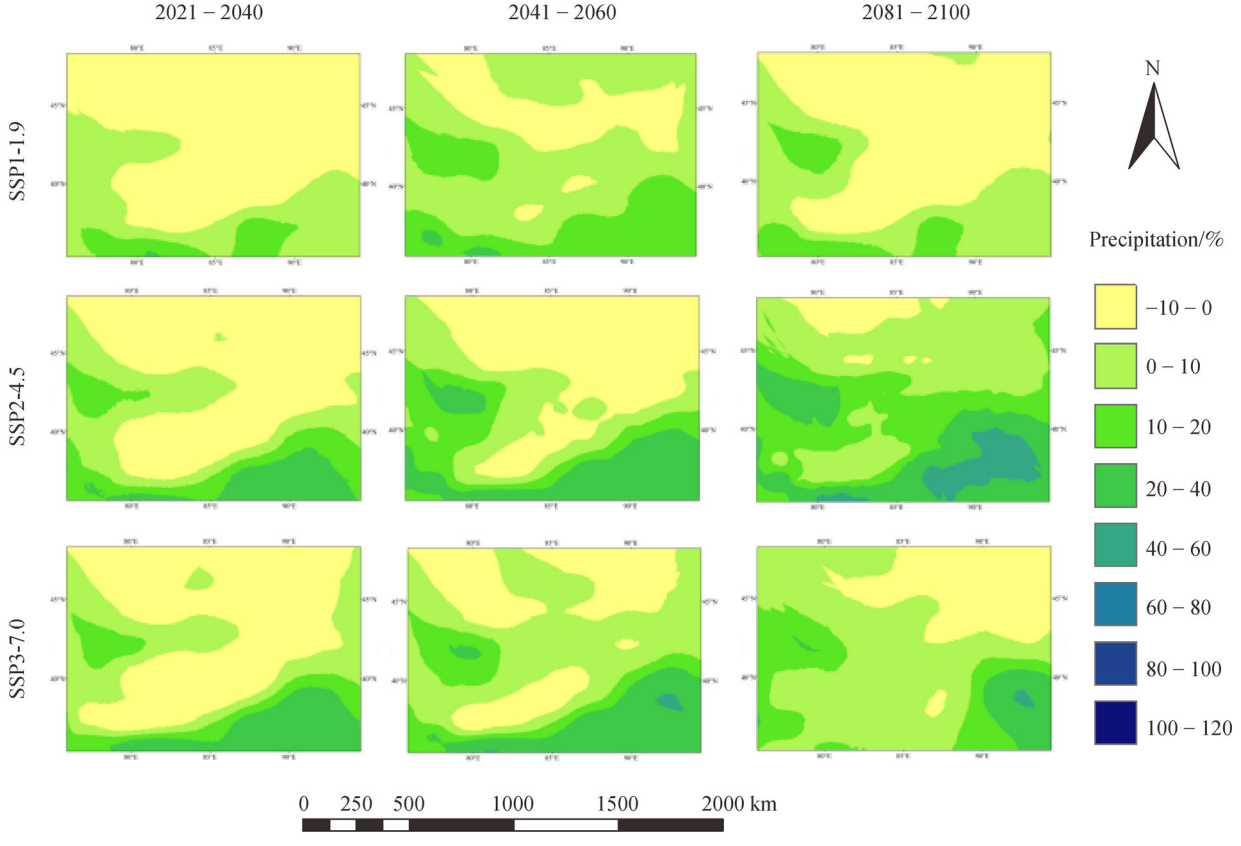

Fig. 11 Spatial patterns of summer precipitation changes in periods of 2021–2040, 2041–2060 and 2081–2100 relative to the reference period (1995–2014) under SSP1-1.9, SSP2-4.5 and SSP3-7.0.

RCP 5-8.5 scenario will be significantly higher than the other scenarios. Change of warming may be due to the increase in greenhouse gas in the atmosphere, which is mainly affected by human activities. At the same time, there is also a good correspondence between the temperature rise and the change in topography, increase in mountainous areas will be relatively small, and the increase in basin will be large. Greater summer warming in the future may be related to the positive feedback process between future snow cover reduction and temperature (Giorgi et al., 1997; Shi et al., 2010). Furthermore, studies have shown that warming in northwest China is negatively correlated with the elevation, and the temperature rise decreases with the increase in altitude, but the change in temperature rise with amplitude and altitude is not a simple linear relationship (Zhang et al., 2019).Previous studies have shown that the summer precipitation is closely related to the western subtropical jet stream in Junggar Basin (Zhao et al., 2014). The reason is that the main source of water vapor is local, although the water vapor has increased, but the increase in temperature decreases water vapor saturation, thus making the precipitation decrease. Summer precipitation in the Junggar Basin decreased slightly, which is likely related to the divergence of water vapor flux in the westerly zone under the background of future warming. Precipitation in the Tarim Basin is significantly affected by the plateau monsoon and Indian Ocean atmospheric circulation (Zhao et al., 2016). Previous studies also show that the change in summer precipitation is related to the positive anomaly of the height field of the north east lateral potential and the abnormal anti-spin circulation, which results in the significant dispersion of water vapor over the Tian Shan mountains and the significant convergence of water vapor over the northern margin of the Kunlun mountains (La et al., 2019). Changes in precipitation are closely related to the 500 hPa circulation anomalies. The southerly airflow in the Junggar Basin region is strengthened, showing an anti-cyclonic circulation, while the northerly airflow in the Tarim Basin region is significantly strengthened, showing a cyclonic circulation, which leads to the increase in precipitation in the southern mountain in summer (Yu et al., 2017).

We found that precipitation will show an increasing trend during the 21st century, this may alleviate the water pressure and be conducive to the agricultural development and environmental restoration of northwest China, because there are great uncertainties in the current GCMs simulation and the future precipitation prediction should be carefully interpreted (Fang et al., 2013).

6 Conclusions

Based on GCMs model outputs from CMIP6 under SSPs-RCPs, future changes in temperature and precipitation over northwest China is analyzed at both annual and seasonal scales. The major findings are as follows:

1) For temperature, results suggest an increase in annual mean temperature. The warming tendency for the period from 2021 to 2100 will be 0.18°C/10a for SSP1-1.9, 0.22°C/10a for SSP1-2.6, 0.31°C/10a for SSP2-4.5, 0.43°C/10a for SSP3-7.0, 0.27°C/10a for SSP4-3.4, 0.34°C/10a for SSP4-6.0, and 0.47°C/10a for SSP5-8.5. In the near-term, spatial patterns of temperature increase will be substantially similar under SSPs-RCPs. In the long term, warming will be 1.4°C for SSP1-1.9, 1.9°C for SSP1-2.6, 3.3°C for SSP2-4.5, 5.5°C for SSP3-7.0, 2.7°C for SSP4-3.4, 3.8°C for SSP4-6.0, and 6.0°C for SSP5-8.5. Spatially, a consistent warming pattern is observed, with the northern part greater than the south. Future warming shows visible seasonal variation with the larger warming in summer and autumn. Maximum warming will be in the mountain areas of the south in spring and autumn, in the southern basins in winter, and in the east in summer.

2) The linear trend in precipitation will be 0.7%/10a for SSP1-1.9, 1.6%/10a for SSP1-2.6, 2.5%/10a for SSP2-4.5, 3.2%/10a for SSP3-7.0, 0.5%/10a for SSP4-3.4, 0.7%/10a for SSP4-6.0, and 2.11%/10a for SSP5-8.5 during 2021–2100. In the long term, increase in precipitation will be significant higher than the near and mid-terms. In the long term, annual precipitation will increase 4.1% for SSP1-1.9, 13.9% for SSP1-2.6, 28.4% for SSP2-4.5, 35.2% for SSP3-7.0, 6.9% for SSP4-3.4, 8.9% for SSP4-6.0, and 27.3% for SSP5-8.5 relative to 1995–2014. Increase in precipitation will be higher in southern Xinjiang than that the north, and especially higher in the mountainous region than the basins under SSP2-4.5, SSP3-7.0, and SSP5-8.5. Seasonally, increase in winter precipitation will be the largest, followed by spring, with significant rise in mountainous regions of southern Tarim Basin. Precipitation increase in winter will be several times than that of other seasons during the same period. Summer precipitation will reduce in Tian Shan and basins, but will increase in the northern margin of the Kunlun significantly.

In the near, mid-, and long-terms, increase in precipitation will alleviate the drying tendency yielded by surface warming. Consequently, the environmental, ecological, and socioeconomic conditions in northwest China will be significantly affected by changing temperature and precipitation, and more efficient mitigation and adaptation strategies need to be carried out to address the impact of future climate change.

Acknowledgements This study was financially supported by the National Key Research and Development Program of China (No. 2018FY100501), National Natural Science Foundation of China (Grant No. 41971023) and CAS "Light of West China" Program (2019-XBQNXZ-B-004).

References

Chen F, Huang W, Jin L, Chen J, Wang J (2011). Spatiotemporal

precipitation variations in the arid central Asia in the context of global warming. Sci China Earth Sci, 54(12): 1812–1821

Chen Y, Liu A, Cheng X (2020). Quantifying economic impacts of climate change under nine future emission scenarios within CMIP6. Sci Total Environ, 703(10): 134950

Cheng D, Wang X (2006). Changing trend of drought and drought disaster in northwest China and countermeasures. Earth Sci Frontiers, 13(1): 3–14 (in Chinese)

Eyring V, Bony S, Meehl G A, Senior C A, Stevens B, Stouffer R J, Taylor K E (2016). Overview of the coupled model intercomparison project phase 6 (CMIP6) experimental design and organization. Geosci Model Dev, 9(5): 1937–1958

Fang S, Yan J, Che M, Zhu Y, Liu Z, Pei H, Zhang H, Xu G, Lin X (2013). Climate change and the ecological responses in Xinjiang, China: model simulations and data analyses. Quat Int, 311: 108–116

He J, Zhang M, Wang P, Xin H, Huang X (2011). New progress of the study on climate change in Xinjiang. Arid Zone Research, 28(3): 499–505 (in Chinese)

Hsiang S M, Meng K C, Cane M A (2011). Civil conflicts are associated with the global climate. Nature, 476(7361): 438–441

Hu R, Fan Z, Wang Y, Yang Q, Huang Y (2001). Assessment about the impact of climate change on environmental in Xinjiang since the recent 50 years. Arid land geography, 24 (2):97–103 (in Chinese)

Hu Z, Yang S, Wu R (2003). Long-term climate variations in China and global warming signals. J Geophys Res, 108 (19) Doi: 10.1029

Hulme M (1996). Recent climatic change in the world's drylands. Geophys Res Lett, 23(1): 61–64

Gao X, Shi Y, Zhang D, Wu J, Giorgi F, Ji Z, Wang Y (2012). Uncertainties in monsoon precipitation projections over China: results from two high-resolution RCM simulations. Clim Res, 52: 213–226

Giorgi F, Hurrell W, Marinucci R, Beniston M (1997). Elevation dependency of the surface climate change signal. J Clim, 10(2): 288–296

IPCC (2013). Climate Change 2013: the Physical Science Basis. Cambridge and New York: Cambridge University Press

Jiang D, Su M, Wei R (2009). Variation and projection of drought and wet conditions in Xinjiang. China J Atmos Sci, 1(33): 90–98 (in Chinese)

La M, Zhou Y, Zhu H, Dong X (2019). On the precipitation changes over Xinjiang in summers from 2006 to 2035 through the dynamical downscaling of CMIP5 model results. J Meteorol Sci, 3(39): 413–420 (in Chinese)

Li B, Chen Y, Chen Z, Li W (2012a). Trends in runoff versus climate change in typical rivers in the arid region of northwest China. Quat Int, 282(19): 87–95

Li H, Sheffield J, Wood E F (2010a). Bias correction of monthly precipitation and temperature fields from Intergovernmental Panel on Climate Change AR4 models using equidistant quantile matching. J Geophys Res-OCEANS, 115(D10): D10101

Li L, Bai L, Yao Y, Yang Q (2012b). Projection of Climate Change in Xinjiang under IPCC SRES. Resources Science, 34(3): 602–612 (in Chinese)

Li Z, Chen Y, Shen Y, Liu Y, Zhang S (2013). Analysis of changing pan evaporation in the arid region of Northwest China. Water Resour Res, 49(4): 2205–2212

Li Q, Dong W, Li W, Gao X, Lones P, Kennedy J, Parker D (2010b). Assessment of the uncertainties in temperature change in China during the last century. Chin. Sci. Bull, 55: 1974–1982

Liu Y, Huang G, Huang R (2011). Inter-decadal variability of summer rainfall in Eastern China detected by the Lepage test. Theor Appl Climatol, 106(3–4): 481–488

Lin P, Yu Z, Liu H, Yu Y, Li Y, Jiang J, Xue W, Chen K, Yang Q, Zhao B, Wei J, Ding M, Sun Z, Wang Y, Meng Y, Zheng W, Ma J (2020). LICOM model datasets for the CMIP6 ocean model intercomparison project. Adv Atmos Sci, 37(3): 239–249

Ma Y, Chen W, Feng R, Liang J, Liang Y (2012). Interannual and interdecadal variations of precipitation over eastern China during Meiyu season and their relationships with the atmospheric circulation and SST. Chin J Atmos Sci, 2: 397–410 (in Chinese)

Meinshausen M, Nicholls J, Lewis J, Gidden J, Vogel E, Freund M, Beyerle U, Gessner C, Nauels A, Bauer N, Canadell J, Daniel S, John A, Krummel B, Luderer G, Meinshausen N, Montzka A, Rayner J, Reimann S, Smith J, van den Berg M, Velders G J M, Vollmer M K, Wang R H J (2020). The shared socio-economic pathway (SSP) greenhouse gas concentrations and their extensions to 2500. Geosci Model Dev, 13(8): 3571–3605

Na Y, Fu Q, Kodama C (2020). Precipitation probability and its future changes from a global cloud-resolving model and CMIP6 simulations. J Geophys Res Atmos, 125(5)

Piao S, Ciais P, Huang Y, Shen Z, Peng S, Li J, Zhou L, Liu H, Ma Y, Ding Y, Friedlingstein P, Liu C, Tan K, Yu Y, Zhang T, Fang J (2010). The impacts of climat e change on water resources and agriculture in China. Nature, 467(7311): 43–51

Shi Y, Gao X, Wu J, Giorgi F, Dong W (2010). Simulation of the changes in snow cover over china under global warming by a high resolution RCM. Journal of Glaciology and Geocryology, 32(2): 215–222 (in Chinese)

Shi Y, Shen Y, Hu R (2003). Preliminary study on signal, impact and foreground of climatic shift from warm-dry to warm-humid in northwest China. Journal of Glaciology and Geology, 24 (3): 219–226(in Chinese)

Shi Y, Shen Y, Kang E, Li D, Ding Y, Zhang G, Hu R (2007). Recent and future climate change in northwest China. Clim Change, 80(3–4): 379–393

Su B, Huang J, Gemmer M, Jian D, Tao H, Jiang D, Zhao C (2016). Statistical downscaling of CMIP5 multi-model ensemble for projected changes of climate in the Indus River Basin. Atmo Res, (178–179):138–149.

Tao H, Fischer T, Su B, Mao W, Jiang T, Fraedrich K (2017). Observed changes in maximum and minimum temperatures in Xinjiang autonomous region, China. Int J Climatol, 37(15): 5120–5128

Tian D, Guo Y, Dong W (2015). Future changes and uncertainties in temperature and precipitation over China based on CMIP5 models. Adv Atmos Sci, 32(4): 487–496

Tokarska K B, Stolpe M B, Sippel S, Fischer E M, Simth C J (2020). Past warming trend constrains future warming in CMIP6 models. Sci Adv, 6(12)

Wang Y, Yang X, Zhang M, Zhang L, Yu X, Ren L, Liu Y, Jiang S, Yuan F (2019). Projected effects of climate change on future hydrological regimes in the Upper Yangtze River Basin, China. Adv Meteorol, 2019: 1–14

Wei F Y (1999). Modern climate statistical diagnostics and prediction technologies. Beijing: China Meteorological Press (in Chinese)

Wu J, Gao X (2013). A gridded daily observation dataset over China region and comparison with the other datasets. Chinese. J Geophysch, 56(4): 1102–1111(in Chinese)

Xu C, Xu Y (2012). The projection of temperature and precipitation over China under RCP scenarios using a CMIP5 multi-model ensemble. Atmos Ocean Sci Lett, 5(6): 527–533

Yang X, Wood E, Sheffield J, Ren L, Zhang M, Wang Y (2018). Bias correction of historical and future simulations of precipitation and temperature for China from CMIP5 models. J Hydrol (Amst), 3(19): 609–623

Yu E, Sun J, Lv G, Chen H, Xiang W (2015). High-resolution projection of future climate change in the northwestern arid regions of China. Arid Land Geography, 38(3): 429–437 (in Chinese)

Yu X, Li S, Zhou Y, Yao J, Li H (2017). Projected summer precipitation over Xinjiang by Multi-CMIP5 models in the next 30 years. Desert and Oasis Meteorology, 11(11): 53–62 (in Chinese)

Zhang Y, Tuerxunban G, Su L, Liu Q (2019). Spatial and temporal characteristics of climate change at different altitudes in Xinjiang in the past 60 years. Arid land geography, 42(4): 822–829 (in Chinese)

Zhao Y, Huang A, Zhou Y, Yang Q (2016). The impacts of the summer plateau monsoon over the Tibetan Plateau on the rainfall in the Tarim Basin, China. Theor Appl Climatol, 126(1–2): 265–272

Zhao Y, Wang M, Huang A, Li H, Huo W, Yang Q (2014). Relationships between the West Asian subtropical westerly jet and summer precipitation in northern Xinjiang. Theor Appl Climatol, 116(3–4): 403–411

Zhou T, Yu R (2006). Twentieth-century surface air temperature over China and the globe simulated by coupled climate models. J Climate, 19: 5843–5858

Zhou J, Wang Y, Su B, Wang A, Tao H, Zhai J, Kundzewicz Z W, Jiang T (2020). Choice of potential evapotranspiration formulas influences drought assessment: a case study in China. Atmos Res, 242: 104979

Zhu B, Xue L, Wei G, Zhang L, Chen X (2019). CMIP5 projected changes in temperature and precipitation in arid and humid basins. Theor Appl Climatol, 136(3–4): 1133–1144